https://doi.org/10.1142/9789811280184_0018

Chapter 18

High Luminosity Forward Physics

M. Deile* and M. Taševský†

*CERN, 1211 Genève 23, Switzerland
†FZU - Institute of Physics of the Czech Academy of Sciences,
Na Slovance 2, 18221 Prague, Czech Republic

1. Introduction

Forward physics and experimentation at the LHC are innovative areas that test the Standard Model more extensively and may unravel new physics, including new Higgs physics. The HL-LHC, expected to provide about ten times more integrated luminosity than collected in Runs 1–3, offers a unique opportunity for detailed studies of central production — a part of forward physics promising from the view of discovery potential — consisting of exclusive and semi-exclusive processes. In these rare events, signals of new physics can emerge through advantageous signal-to-background ratios thanks to the additional kinematic information (compared to inclusive processes) in conjunction with keeping combinatorial backgrounds from high pile-up under control. For the latter, timing detectors with excellent resolutions are crucial.

The central (semi-) exclusive production processes in proton-proton collisions, $pp \to p \oplus X \oplus p$, are defined by one intact proton on each side of the interaction point (IP), a state X produced at central rapidities and (almost) no other activity in the central detector, manifesting itself in large rapidity gaps (LRG, denoted by $\oplus$). The intact protons are characterized by very small scattering angles relative to the beam and by small momentum losses, $\Delta p_{1/2}$, of proton 1 on one side and proton 2 on the other side of the IP with respect to the momentum p of the incoming proton,

permitting the creation of the central state X. The fractional momentum loss, $\xi_{1/2} := \Delta p_{1/2}/p$, typically amounts to only a few percent. Thus these protons stay very close to the beam and escape the central detector. They are measured by dedicated forward proton detectors (FPD) that need to be placed far from the IP and very close to the circulating beam (a few millimeters away).

Already in the first two LHC runs — and to be continued in Run 3 — both interaction points IP1 and IP5 have been equipped with FPDs, first pioneered by TOTEM [1] and ATLAS-ALFA [2] for measurements of elastic and soft diffractive scattering in special runs. In Long Shutdown LS1, these systems were complemented and upgraded for high luminosity operation in all regular LHC runs, yielding the ATLAS-AFP [3] and CMS-PPS [4] (initially CMS-TOTEM PPS) subdetectors dedicated to measurements of processes with much lower cross sections than the ones of elastic and soft diffractive scattering. Both spectrometers are equipped with trackers to measure kinematic quantities and time-of-flight (ToF) detectors to measure proton arrival times, the latter enabling the reconstruction of the longitudinal vertex position, which is essential at the high pile-up levels of LHC, even more so at the HL-LHC. Both are also an integral part of the data acquisition system and central trigger of the main detectors.

During the Long Shutdown LS3, the Long Straight Sections LSS1 and LSS5 will be redesigned and the present AFP and PPS systems uninstalled. This offers an opportunity to develop improved detector systems and to place them in optimised locations, building on the experience gained in the first LHC runs (see Refs. [5] and [6] for more details).

2. Physics Objectives

The experimental signature of (semi-) exclusive processes are usually explained by an exchange of a colourless object with vacuum quantum numbers between the colliding particles. This object can be a gluonic state (Pomeron) or a photon. Pomeron (photon) exchanges dominate at central system masses below (above) roughly 150 GeV.

In the presence of high pile-up, the LRGs are filled by particles from unrelated interactions, and one has to rely on other exclusivity criteria. These include matching at two levels: kinematic quantities and the primary vertex measured by the central detector should equal those measured by the FPD. The requirement on LRGs is then replaced by a track veto: zero or very few tracks are allowed around the primary vertex.

Although double-proton tagging is necessary for the ToF method to work for the FPDs alone, time information can also be provided by the central detector (see HGTD [7] and MTD [8] — fast time detector upgrades for HL-LHC in ATLAS and CMS, respectively), in which case single-tag events are a viable alternative that extends the physics reach to smaller masses and adds single-proton dissociation to the signal processes [9, 10]. This increases the event yield but also leads to a more serious background contamination. Since the background mostly comes from Standard Model (SM) processes, their precise measurements are indispensable in any search for physics beyond the SM (BSM). Published measurements with tagged protons (exclusive and semi-exclusive production of pairs of photons [11], top quarks [14], W and Z bosons [15, 16] and leptons [17, 18]) demonstrated the viability of using FPDs in high pile-up environments and paved the way to measuring even rarer (semi-) exclusive processes with similar final states but in harsher HL-LHC conditions. Phenomenological studies suggest promising prospects for extracting (semi-) exclusive signals of SM processes (e.g. $t\bar{t}$ production [19, 20]) and various BSM processes, even with HL-LHC pile-up levels. Photon-induced processes, for example, give access to anomalous magnetic moments [21], searches for Dark Matter [22, 23], axion-like particles [24], and anomalous gauge couplings [26, 27] studied via Effective Field Theory. On one hand, measuring rates or properties of Higgs bosons (e.g. quantum numbers or the $Hb\bar{b}$ Yukawa coupling [28–30]), born exclusively via Pomeron fusion, can help inclusive analyses to determine the SM or BSM nature of the Higgs boson discovered at a mass of 125.5 GeV. Alternatively, on the other hand, this can potentially shed light on the excess at masses around 95 GeV [31]. Such low masses will be reachable only if detector stations are placed about 420 m from the IP. In general, if deviations from the SM are observed experimentally, a categorised analysis (no-tag, single-tag, double-tag) would be advisable for disentangling different sources of new physics effects.

3. AFP and PPS Proton Spectrometer Layouts at HL-LHC

The search for suitable detector locations is driven by the physics programme striving for the coverage of the widest possible range of masses in diffractive processes. The mass of the central system in (semi-) exclusive processes is obtained via the relation:

$$M^2 = \xi_1 \, \xi_2 \, s \, , \tag{1}$$

where $\sqrt{s} = 14$ TeV is the centre-of-mass energy.

The protons are deflected from the beam centre in a direction determined by the horizontal and vertical dispersion of the LHC bending magnets. They are then detected by sensors approaching the beam in movable beam-pipe insertions, e.g. so-called Roman Pots (RPs). In the case of horizontal beam crossing (to be implemented in IP1), the dispersion is almost purely horizontal, whereas for vertical crossing (to be implemented in IP5) there is also a substantial vertical component. In both cases the best detector acceptance for leading protons with $\xi > 0$ is obtained with sensors approaching the beam horizontally, i.e. along x.

The minimum accessible $|\xi|$ is given by the ratio of the closest detector approach to the beam, defined as a multiple of the horizontal beam width, σ_x, and the horizontal dispersion D_x at that location: $|\xi|_{\min} \propto \sigma_x/|D_x|$. In LSS1 and LSS5, locations with small $|\xi|_{\min}$ lie around the quadrupole Q6 and at distances greater than 300 m from the IP.

Events with large M or ξ have protons moving far away from the beam centre, hence their acceptance is determined by the tightest aperture limitations upstream of the detection point. Since the dominant aperture bottlenecks are the debris collimators (TCLX4, TCL5 and TCL6), it is advantageous to place detector stations immediately upstream of them.

A layout solution taking into account these acceptance considerations and the available space in the beam line is shown in Fig. 1. In both AFP and PPS, detector stations are proposed at ∼196 m (RP1), ∼220 m (RP2), ∼234 m (RP3) and, at a later stage, at ∼420 m (RP4) from the IP, on both sides. Each of these stations will consist of two horizontal detector units with a few meters of lever arm to allow the measurement of track angles.

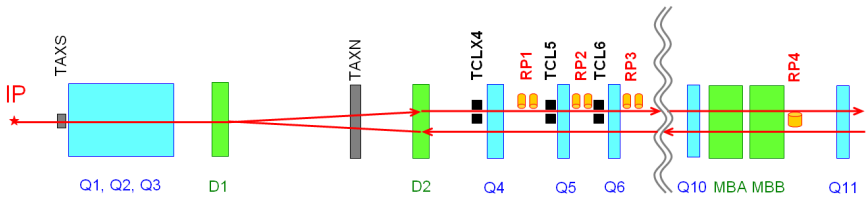

Fig. 1. Schematic overview of the planned AFP/PPS stations in Sector 1-2 / 5-6 (outgoing Beam 1) (adapted from Ref. 32). The dipoles (D1, D2, MBA, MBB), quadrupoles (Qn) and higher order correctors (not shown) define the beam optics. TAXS and TAXN are shower absorbers. The instrumentation in Sector 8-1 / 4-5 (outgoing Beam 2) is mirror-symmetric.

4. Kinematic Acceptance

The central mass acceptance for a generic central diffractive process, where the mass in double-tag events is evaluated using Eq. (1), varies over a fill because the luminosity levelling procedure [33] gradually changes the beam optics determining the proton trajectories from the IP to the detectors. During most of the fill, for optics characterized by β^{*}[a] values between 50 and 15 cm, the variations of the mass limits amount to only a few tens of GeV. On average, PPS will reach the mass intervals (1150, 2750), (500, 900) and (200, 350) GeV for the stations RP1, RP2 and RP3, respectively. For AFP, due to a lower horizontal dispersion, the horizontal crossing scheme in IP1 leads to substantially higher masses compared to the vertical crossing in IP5, the corresponding intervals are: (2000, 5000), (1000, 4000), (600, 1600) GeV. The stations RP4, envisaged for a later stage, will add acceptance at low masses in the region (50, 160) GeV. The single-tag configuration in general leads to the mass minimum of a few tens of GeV. The exact value is given by the kinematical limit and central detector acceptance for a given process.

5. Instrumentation

5.1. *Movable Detector Vessels*

For the locations up to 245 m from the IPs, the well-proven Roman Pot technology is an adequate solution for housing the detectors and moving them towards the beam. Only details (size and shape) of the detector chambers need to be adapted to the expected hit distributions at HL-LHC in each location. Each pot will contain a stack of tracking and timing detectors. The strongly peaked radiation near the beam will lead to local fluences up to 10^{16} p/cm^2 after an integrated luminosity of 300 fb^{-1}, which can be reached within a year of running. Such fluence peaks are currently beyond the radiation hardness of most detector and readout electronics technologies. The local radiation damage is mitigated by periodic vertical displacements of the detector package, which distributes the irradiation over the detectors. This principle has been successfully tested in Run 2 by raising or lowering entire RP units relative to the beam centre in short technical stops during the running seasons [34]. At HL-LHC, however, it is expected that the harsh radiation will limit tunnel accesses to only

[a] β^{*} is the value of the betatron function at the IP.

regular End-of-Year technical stops. Therefore, remote-controlled vertical movement systems have been developed and will be tested in Run 3.

The RP location RP4 at 420 m, considered for a later stage, would be substantially different from the others: since the horizontal dispersion has the opposite sign, the signal proton tracks will end up in the narrow space between the outgoing and incoming beam pipes, which excludes the conventional RP technology and requires new developments. In addition, this location lies in the cryogenic region and is presently occupied by the empty cryostat LEGR, which would thus have to be replaced with a cryogenic bypass. Possible solutions are explored in cooperation with the collimation team, which has already developed such a bypass for the installation of new TCLD collimators in other interaction regions. Alternatively, one can also make use of solutions developed for the FP420 R&D project and described in great detail in its TDR [35].

5.2. *Detector Technologies*

5.2.1. *Tracking Detectors*

Both AFP and PPS spectrometers base their tracking on a 3D Silicon pixel technology which excels in: i) a very narrow dead area (around 50 μm), ii) very good spatial resolution (sub-10 μm), and iii) radiation hardness. This provides: i) detector efficiency as close as possible to the beam (maximizing the mass acceptance), ii) precise measurement of the central system mass and iii) tolerance of high radiation levels. Both projects plan to maintain this technology for HL-LHC.

The 3D Silicon sensors to be used in Run 3 by AFP [36, 37] and PPS [34, 38, 39] are segmented in pixels of (50×250) μm^2 and (100×150) μm^2, respectively, and are expected to withstand radiation doses of up to 5×10^{15} p/cm^2. Smaller pixel cells with higher radiation tolerance have been successfully tested for HL-LHC conditions [40].

5.2.2. *Timing Detectors*

ToF detectors were first installed in Run 2 by both AFP and PPS. While AFP used a matrix of 16 L-shaped *quartz bars* with the smallest transverse size of 2 mm, detecting Cherenkov light [41], PPS instead relied on single crystal Chemical Vapour Deposit (scCVD) *diamond detectors* in "double diamond" readout configuration [34, 42] with a crystal size of (4.5×4.5) mm^2. Low pile-up runs and testbeam measurements demonstrated time

resolutions of 20–30 ps and 50 ps for the quartz bars and the double-diamond plane, respectively. From the point of view of the long-term LHC operation, both systems suffered radiation damage to their readout chains.

A pile-up multiplicity of 200 interactions per bunch crossing, as expected ultimately at HL-LHC, leads to a vertex density of about 1.5/mm at $z = 0$ (where this density is highest) [7] and up to 3 protons ending up in the FPD acceptance. To reduce this combinatorial background, equipping FPD with a ToF detector with a resolution of the order of 10 ps and a granularity of 1 mm seems to be imperative [43]. An additional improvement will come from the combination of ToF information from the FPD and the central detector (see HGTD [7] and MTD [8]).

There are presently three viable ToF detector options in R&D phases and on good track to attain the required resolution and granularity: Quartz bars and diamonds as described above, along with radiation-hard read-out electronics, and Low Gain Avalanche Diodes (LGAD). The latter were developed for the CMS Endcap Timing Layer [8, 44] and for HGTD [7], making them a conceivable option for AFP and PPS with maximum synergy inside the respective collaborations. Similar to the tracker, the non-uniform irradiation would be tackled by moving the whole detector package according to the fluence.

References

[1] The TOTEM Collaboration, The TOTEM Experiment at the CERN Large Hadron Collider, JINST. **3**, S08007 (2008).
[2] S. Abdel Khalek et al., The ALFA Roman Pot Detectors of ATLAS, JINST. **11**(11), P11013 (2016).
[3] L. Adamczyk et al. Technical Design Report for the ATLAS Forward Proton Detector. CERN-LHCC-2015-009; ATLAS-TDR-024 (2015).
[4] The CMS and TOTEM Collaborations. CMS-TOTEM Precision Proton Spectrometer. CERN-LHCC-2014-021; TOTEM-TDR-003; CMS-TDR-13 (2014).
[5] The CMS Collaboration. The CMS Precision Proton Spectrometer at the HL-LHC – Expression of Interest. arXiv:2103.02752.
[6] L. Adamczyk et al. Initial Design Report for the ATLAS Forward Proton Detector, in preparation. (2022).
[7] G. Aad et al. Technical Design Report: A High-Granularity Timing Detector for the ATLAS Phase-II Upgrade. CERN-LHCC-2020-007 (2020).
[8] The CMS Collaboration. A MIP Timing Detector for the CMS Phase-2 Upgrade. CERN-LHCC-2019-003; CMS-TDR-020 (2019).

[9] L. A. Harland-Lang et al., A new approach to modelling elastic and inelastic photon-initiated production at the LHC: SuperChic 4, Eur. Phys. J. C. **80**(10), 925 (2020).
[10] S. Bailey et al. Modelling W^+W^- production with rapidity gaps at the LHC. arXiv:2201.08403 (2022).
[11] A. Tumasyan et al., First Search for Exclusive Diphoton Production at High Mass with Tagged Protons in Proton-Proton Collisions at $\sqrt{s} = 13$ TeV, Phys. Rev. Lett. **129**(1), 011801 (2022). doi: 10.1103/PhysRevLett.129.011801.
[12] The CMS and TOTEM Collaborations, Search for exclusive diphoton production with intact protons in PPS, CMS-PAS-EXO-21-007; TOTEM-NOTE-2022-005 (2022) `https://cds.cern.ch/record/2810862`.
[13] Aad, Georges and others, Search for an axion-like particle with forward proton scattering in association with photon pairs at ATLAS, arXiv 2304.10953, CERN-EP-2023-049 (2023).
[14] The CMS and TOTEM Collaborations. Search for central exclusive production of top quark pairs in proton-proton collisions at $\sqrt{s} = 13$ TeV with tagged protons. CMS-PAS-TOP-21-007; TOTEM-NOTE-2022-002 (2022). URL `https://cds.cern.ch/record/2803843`.
[15] Search for high-mass exclusive $\gamma\gamma \to$ WW and $\gamma\gamma \to$ ZZ production in proton-proton collisions at $\sqrt{s} = 13$ TeV (11, 2022).
[16] A search for new physics in central exclusive production using the missing mass technique with the CMS detector and the CMS-TOTEM precision proton spectrometer (3, 2023).
[17] G. Aad et al., Observation and Measurement of Forward Proton Scattering in Association with Lepton Pairs Produced via the Photon Fusion Mechanism at ATLAS, Phys. Rev. Lett. **125**(26), 261801 (2020).
[18] The CMS and TOTEM Collaborations, Observation of proton-tagged, central (semi)exclusive production of high-mass lepton pairs in pp collisions at 13 TeV with the CMS-TOTEM precision proton spectrometer, JHEP. **07**, 153 (2018).
[19] V. P. Gonçalves et al., Top quark pair production in the exclusive processes at the LHC, Phys. Rev. D. **102**(7), 074014 (2020).
[20] D. E. Martins, M. Tasevsky, and V. P. Goncalves, Challenging exclusive top quark pair production at low and high luminosity LHC, Phys. Rev. D. **105**(11), 114002 (2022). doi: 10.1103/PhysRevD.105.114002.
[21] L. Beresford and J. Liu, New physics and tau $g-2$ using LHC heavy ion collisions, Phys. Rev. D. **102**(11), 113008 (2020).
[22] L. A. Harland-Lang et al., LHC Searches for Dark Matter in Compressed Mass Scenarios: Challenges in the Forward Proton Mode, JHEP. **04**, 010 (2019).
[23] L. Beresford and J. Liu, Search Strategy for Sleptons and Dark Matter Using the LHC as a Photon Collider, Phys. Rev. Lett. **123**(14), 141801 (2019).
[24] C. Baldenegro et al., Searching for axion-like particles with proton tagging at the LHC, JHEP. **06**, 131 (2018).

[25] L. A. Harland-Lang and M. Tasevsky, New calculation of semiexclusive axionlike particle production at the LHC, arXiv 2208.10526, doi: 10.1103/PhysRevD.107.033001, *Phys. Rev. D* vol. 107(3), p. 033001 (2023).
[26] S. Fichet et al., Light-by-light scattering with intact protons at the LHC: from Standard Model to New Physics, JHEP. **02**, 165 (2015).
[27] E. Chapon et al., Anomalous quartic W W gamma gamma, Z Z gamma gamma, and trilinear WW gamma couplings in two-photon processes at high luminosity at the LHC, Phys. Rev. D. **81**, 074003 (2010).
[28] S. Heinemeyer et al., Studying the MSSM Higgs sector by forward proton tagging at the LHC, Eur. Phys. J. C. **53**, 231–256 (2008).
[29] B. E. Cox et al., Detecting Higgs bosons in the $b\bar{b}$ decay channel using forward proton tagging at the LHC, JHEP. **10**, 090 (2007).
[30] M. Tasevsky, Review of Central Exclusive Production of the Higgs Boson Beyond the Standard Model, Int. J. Mod. Phys. A. **29**, 1446012 (2014).
[31] T. Biekötter et al. Mounting evidence for a 95 GeV Higgs boson. arXiv:2203.13180 (3, 2022).
[32] J. Oliveira et al. Layouts of HL-LHC Insertions - IR5, IR6, IR7, IR8, drawing LHCLSXGH0002 v.AB, EDMS 1557086 (2020).
[33] G. Arduini et al. HL-LHC Run 4 proton operational scenario. CERN-ACC-2022-0001 (2022). URL `https://cds.cern.ch/record/2803840`.
[34] The CMS Collaboration. The evolution and performance of the CMS detector at the CERN LHC, Chapter 6. PRF-21-001 (2022).
[35] M. G. Albrow et al., The FP420 R&D Project: Higgs and New Physics with forward protons at the LHC, JINST. **4**, T10001 (2009).
[36] J. Lange et al., 3D silicon pixel detectors for the ATLAS Forward Physics experiment, JINST. **10**(03), C03031 (2015).
[37] J. Lange et al., 3D silicon pixel detectors for the High-Luminosity LHC, JINST. **11**(11), C11024 (2016).
[38] F. Ravera, The CT-PPS tracking system with 3D pixel detectors, JINST. **11**(11), C11027 (2016).
[39] M. M. Obertino, The PPS tracking system: performance in LHC Run2 and prospects for LHC Run3, JINST. **15**(05), C05049 (2020).
[40] S. Terzo et al., A new generation of radiation hard 3D pixel sensors for the ATLAS upgrade, Nucl. Instrum. Meth. A. **982**, 164587 (2020).
[41] L. Chytka et al., Timing resolution studies of the optical part of the AFP Time-of-flight detector, Optics Express. **26(7)**, 8028–8039 (2018).
[42] E. Bossini, The CMS Precision Proton Spectrometer timing system: performance in Run 2, future upgrades and sensor radiation hardness studies, JINST. **15**(05), C05054 (2020).
[43] K. Černý et al., Performance studies of Time-of-Flight detectors at LHC, JINST. **16**(01), P01030 (2021).
[44] M. Ferrero, The CMS MTD Endcap Timing Layer: Precision timing with Low Gain Avalanche Diodes, Nucl. Instr. Meth. A. **1032**, 166627 (2022).